Transport and EPR studies of polyaniline: A quasi-one-dimensional conductor with three-dimensional "metallic" states

Z. H. Wang*
Department of Physics, The Ohio State University, Columbus, Ohio 43210

E. M. Scherr and A. G. MacDiarmid
Department of Chemistry, University of Pennsylvania, Philadelphia, Pennsylvania 19104

A. J. Epstein
Department of Physics, The Ohio State University, Columbus, Ohio 43210
and Department of Chemistry, The Ohio State University, Columbus, Ohio 43210
(Received 13 September 1991)

It is an open question if "metallic" polymers have one-dimensional or three-dimensional conduction states. We investigate this issue by studying a model polymer, the HCl-doped emeraldine salt form of oriented polyaniline (PAN-ES) through the temperature dependence of the dc conductivity, thermoelectric power, complex microwave dielectric constant, electron paramagnetic resonance (EPR), and electric-field dependence of conductivity. The thermopower, microwave dielectric constant, and EPR data suggest that the electrons are three dimensionally delocalized. We propose that oriented PAN-ES consists of coupled parallel chains that form "metallic" bundles. These bundles are the "crystalline" regions of the polymer in which the electron wave functions are three dimensionally extended. This is in contrast to conventional quasi-one-dimensional conductors (many "metallic" charge-transfer salts) in which conducting chains are essentially isolated. However, between bundles are the amorphous (less-ordered) regions in which charge hopping dominates the macroscopic conductivity. The formation of the "metallic" bundles is proposed to be the result of a significant charge-interchain-transfer rate inside the crystalline regions. The implications of the results for the improvement of conductivity are addressed.

I. INTRODUCTION

Disordered quasi-one-dimensional (quasi-1D) conductors have been extensively investigated in the past three decades.[1-6] Among examples of the quasi-1D conductors are various charge-transfer salts of tetracyanoquinodimethane (TCNQ). The common feature of these materials, among others, is that electrons transport mainly along one-dimensional chains, with resultant large anisotropy of conductivities,[1,2] (positive) dielectric constants,[3,4] thermoelectric powers,[5] and optical reflectance.[1,6] In these materials "metallic" behaviors were found only along the highly conducting axis. For example, the low-temperature microwave dielectric constant of tetrathiofulvalene TCNQ, or TTF TCNQ, was found to on the order of 10^3 along the highly conducting axis, while only approximately 6 in the transverse direction.[4] Metallic thermoelectric power[1,2,5] and "Drude" absorption[1,6] only exist in the highly conducting direction. Therefore, these materials are believed to be composed of many essentially isolated metallic chains and electrons transport along the chains with interchain hopping as a necessary secondary step.

Heavily doped conducting polymers are another class of quasi-1D materials. It is generally assumed that electrons are also transporting primarily along the polymer chains[7] and it has been observed that the conductivity,[8] optical reflectance,[9] and magnetoconductivity[10] of the oriented "metallic" polymers are highly anisotropic. Models based on the assumption that each polymer chain is an isolated one-dimensional conductor have been proposed to account for many experimental observations[11] while the important role of interchain charge motion has been noted.[12]

However, it is still not clear if these metallic polymers are 1D conductors. There are two intrinsic phenomena associated with a one-dimensional system. One is the electron localization in a strictly 1D-disordered system with any weak disorder.[3,13] This phenomenon plays an important role in many 1D conductors, including some TCNQ salts.[3] Since there is extensive disorder and large amounts of dopants or impurities in the polymers, 1D localization is expected to have dramatic impact. This, however, is not the case for some conducting polymers. For example, doped polyacetylene has conductivity as high as $\sim 10^5$ S/cm, close to that of copper at room temperature.[8,14,16] The electron states are obviously extended since the mean free path l_i of electrons is estimated to be as long as 600 Å,[8,10,16] a well-defined extended state. Another phenomenon is the Peierls instability at low temperatures;[1] a one-dimensional system is not stable against periodic lattice distortion which opens a gap, known as "Peierls gap," at the Fermi energy at low temperatures. The 1D system thus becomes an insulator.[1] This is the case for many TCNQ salts and other similar one-dimensional conductors.[1,2] For some charge-transfer

salts there is sufficient 3D coupling to suppress the Peierls transition and even stabilize a superconducting state.[1] In contrast to the TCNQ and similar quasi-1D charge-transfer salts, the metallic state of conducting polymers seems stable at any temperature. Experiments have been performed to as low as 10 mK for doped polyacetylene without observing any Peierls instability.[8,15] Thus Kivelson and Heeger suggested, among other things, that the interchain coupling could be important for heavily doped polyacetylene in suppressing the Peierls instability and avoiding the 1D localization.[16] Javadi *et al.* further pointed out, based on their magnetoresistance studies, that 3D metallic states may be formed in metallic polyacetylene.[10] Others proposed that polyacetylene *fibrils* observed by electron microscopic are the "metallic" conductors based on which they analyzed the transport data of polyacetylene.[17] However, these suggestions are principally conjectures. Until now experimental studies of conducting polymers have been inadequate to determine the dimensionality of their conducting states with results being ambiguous even for $(CH)_x$.[7-12,14-18] Detailed studies of the anisotropy of the conducting polymers are essential to the determination of the dimensionality of the conducting states and hence the origin of their high conductivity as well as the mechanism for stabilization of their "metallic" states.

In this paper we present the transport and magnetic studies of one *model* "metallic" conducting polymer, the HCl-doped emeraldine salt form of oriented polyaniline (PAN-ES), including temperature dependence of its dc conductivity, microwave frequency conductivity and dielectric constant, thermoelectric power, electric-field dependence of conductivity, and electron paramagnetic resonance (EPR). Some results have been briefly reported previously.[19]

Polyaniline is selected as a model system because (1) it is stable in both pristine emeraldine base (PAN-EB) and fully doped emeraldine salt (PAN-ES) forms; (2) the relevant polyaniline chemistry for doping is understood.[20] The conclusions we draw from study of the polyaniline system are general and likely applicable to other metallic polymers. PAN-ES itself is a controversial polymer with respect to the nature of its electron states (metallic or localized).[21] Based on earlier transport and magnetic studies of PAN-ES which showed thermopower $S(T) \propto T$, conductivity $\sigma(T) \propto \exp[-(T_0/T)^{1/2}]$, and linearly increasing Pauli-like susceptibility with doping concentration, PAN-ES was proposed to be a (3D) granular metal.[22] However, Lundberg, Salaneck, and Lundstrom suggested,[23] from the electric-field and pressure dependences of conductivity, that the electron states in PAN-ES are localized and that the conductivity is due to quasi-1D variable-range hopping (VRH). Wudl *et al.* considered[24] PAN-ES as a Fermi glass system motivated by its relatively high-Curie spin concentration. A more detailed study was performed by Mizoguchi, Nechtschein, and co-workers utilizing frequency-dependent EPR and NMR measurements of PAN-ES.[25] They found, on the one hand, that the intrachain spin diffusion rate of PAN-ES is independent of doping concentration. This they considered in terms of a granular metal model, although they proposed that the metallic grains are isolated "single conducting chains." On the other hand, the value of intrachain diffusion rates is too low to be metallic at all. Therefore, it is still an open question whether the conduction states of PAN-ES are metallic or localized.

We propose that oriented PAN-ES represents a class of quasi-1D disordered conductors consisting of bundles of well-coupled chains in which electron states are three-dimensionally (3D) extended, different from conventional 1D conductors which consist of essentially isolated chains.[1-6] These 3D metallic bundles correspond to crystalline (or more ordered) regions of the polymer[26] and are separated from one another by the amorphous (or less-ordered) regions (more than 50% of samples is amorphous) of the polymer. The data suggest that the macroscopic conductivity of PAN-ES is dominated by quasi-1D VRH (Refs. 28–30) either in the amorphous regions or between the bundles. Compared with the properties of polyaniline derivative, poly(*o*-toluidine), where interchain coupling and coherence are suppressed,[28] it is demonstrated that the interchain coupling is a key factor in the formation of true metallic polymers. Our experimental results contradict the single conducting chain models.[25] The results also suggest that the improvement of interchain coupling is an important strategy to achieve high conductivity.

This paper is organized as follows: In Sec. II, relevant theoretical models are briefly reviewed. The experimental techniques and results are presented in Sec. III, followed by discussion of the results in Sec. IV. Finally, we conclude our studies in Sec. V.

II. THEORETICAL BACKGROUND

A. 1D localization versus 3D delocalization

It is well known that electron states in a strictly one-dimensional disordered system (1D-DS) are localized with any weak disorder.[3,29] The physical reason for the localization originates from the interference of backward-scattered electron wave functions with forward-electron wave functions forming standing waves and hence localizing the electron states.

The situation for a quasi-one-dimensional disordered system (quasi-1D-DS), where electrons can transfer between the chains, may be quite different. If the electrons can move off the chain before they encounter impurities, the electrons can effectively avoid backward scattering and hence become delocalized. In this case the electrons can transport three dimensionally in the systems.

The interchain transfer rate is a very important parameter in controlling the electron localization in a quasi-1D-DS. Assuming the mean free time of an electron moving along a chain is τ and the interchain transfer rate is w, the condition for an electron to avoid 1D localization is approximately $w > 1/2\tau$ (see below). Therefore, there exists a threshold value of w, $w_c \sim 1/\tau$, above which ($w > w_c$) electron states are extended three dimensionally, below which ($w < w_c$) they are localized to a single chain.

The interchain transfer rate w is a function of the following parameters: interchain exchange integral $t_\perp$, τ,

and interchain mean free time $\tau_\perp$. The rigorous relationship between w and these parameters depends on whether the interchain transfer is coherent or not. Let us consider a simple model. Assuming all the chains are perfectly packed with the principal axis along the z direction and tetragonal in the perpendicular (x,y) directions, the dispersion relation can be written as

$$E(k)=E(k_\perp)+2t_0\cos(k_z c)\ ,$$
$$E(k_\perp)=2t_\perp\cos(k_x a)+2t_\perp\cos(k_y b)\ , \tag{1}$$

where E is the electron energy, $t_0(t_\perp)$ is the in-chain (interchain) transfer integral, (a, b, c) and (k_x, k_y, k_z) are lattice constants and wave vectors in the x, y, z directions. The electron transverse velocity, say v_x, is then given by

$$v_x=\frac{dE(k)}{dk_x}=\frac{2t_\perp a}{\hbar}\sin(k_x a)\ . \tag{2}$$

For a half-filled band, $k_x=\pi/a$ and we obtain

$$v_x=\frac{2t_\perp a}{\hbar}\ . \tag{3}$$

The mean free path l_i is then

$$l_i=v_x\tau=\frac{2t_\perp\tau}{\hbar}a\ . \tag{4}$$

If $l_i>a$, the electron can move from one chain to its nearest-neighboring chains without being scattered; the interchain motion is *coherent*. On the other hand, if $l_i<a$, the interchain motion is *incoherent*. So $2t_\perp\tau\approx\hbar$ is the boundary between coherent and incoherent interchain transfer. A similar conclusion has been reached by Jerome and Schulz.[1] For coherent motion, the interchain transfer rate w is

$$w=v_x/a=2t_\perp/\hbar\ . \tag{5}$$

For incoherent motion (diffusion)

$$w=D_\perp a^2=l_i v_x/a^2=4t_\perp^2\tau/\hbar^2\ , \tag{6}$$

where $D_\perp$ is the perpendicular diffusion coefficient.

Let us now consider the condition for 3D delocalization. The electrons moving along a chain will be scattered in time τ and move back to the initial position in time 2τ. In this period if the electrons are still on this chain, forward and backward electron waves will interfere and localize the electrons. Therefore, the approximate condition for 3D delocalization is

$$w>\frac{1}{2\tau}\ . \tag{7}$$

For coherent interchain motion, we get by inserting Eq. (5) into Eq. (7)

$$t_\perp\tau>\hbar/4=0.25\hbar\ . \tag{8}$$

For incoherent motion, the condition becomes

$$t_\perp\tau>\hbar/2^{3/2}=0.35\hbar\ . \tag{9}$$

We can see that the 3D delocalization condition is more easily fulfilled for coherent interchain motion.

If the polymer chain packing is not perfect, interchain disorder will reduce w and hence probably localize the electron wave functions. Assuming interchain mean free time $\tau_\perp$, we obtain

$$w=\frac{4t_\perp^2\tau'}{\hbar^2}\ , \tag{10}$$

where $(\tau')^{-1}=(\tau)^{-1}+(\tau_\perp)^{-1}$.

A more realistic model for a heterogeneous system like the polyaniline emeraldine hydrochloride polymer is N coupled chains packed into a bundle. The bundles could be the polymer fibers or crystalline regions of the polymers in which chains are well ordered. This system has been studied by Firsov and co-workers theoretically.[13] Their main conclusions are (1) the transverse energy spectrum for interchain motion is discrete: (2) when $w>w_c$, there exists a "zero mode" state (ground state) which corresponds to a homogeneous distribution of electron wave functions over the N chains. The interchain localization length becomes $L_\perp\sim Na$ and the in-chain localization length will be enhanced such that $L_\parallel\sim Nl$ where l is the localization length for a strictly 1D chain. A state is called 3D metallic state if $L_\perp\gg a$ and $L_\parallel\gg c$. This 3D anisotropic metallic state is similar to the states in thin metallic wires where Thouless localization plays an essential role.[31]

B. Transport properties of quasi-1D disordered systems

For 1D localized states, e.g., $w<w_c$, charge transport is dominated by quasi-1D VRH at low temperatures.[28–30] For weak interchain coupling where only the nearest-neighbor chain hopping is considered, interchain conductivity is determined by

$$\sigma_\perp=\sigma_0\exp[-(T_0/T)^{1/2}]\ , \tag{11}$$

where $k_B T_0=16/L_\parallel N(E_F)z$ [$N(E_F)$ is the density of states at the Fermi energy E_F for both signs of spin and z is the number of nearest-neighbor chains]. The in-chain hopping is dominated by the most difficult nearest-neighbor hop which results in a conductivity of the form $\sigma_\parallel\sim\exp(-T_0'/T)$. However, since the pure in-chain motion is more difficult, interchain motion around the most difficult barriers is expected to dominate the temperature dependence of the macroscopic conductivity. Hence the macroscopic $\sigma_\parallel$ is expected to also have the temperature dependence of $\sigma_\parallel\sim\exp[-(T_0/T)^{1/2}]$, with some differences in the T_0 for $\sigma_\parallel$ and $\sigma_\perp$. Note that Eq. (11) could be applied to the interbundle quasi-1D VRH if the metallic bundles are formed (e.g., $w>w_c$), since a bundle may be considered as a large-scale chain.

The hopping conductivity is expected to depend on electric field F. At moderate electric field $eRF\sim k_B T$ (Ref. 29) where R is the hopping distance, we have

$$\sigma(F)\propto\exp(eRF/k_B T)\ . \tag{12}$$

If F is in the chain direction and R is the most probable

hopping distance in the presence of interchain hopping, then[28]

$$R_{\parallel}=\frac{L_{\parallel}}{4}\left[\frac{T_0}{T}\right]^{1/2} \tag{13}$$

If F is perpendicular to the chain direction, $R=a$ for the hopping to the nearest-neighboring chains or $R=L_{\perp}$ for nearest interbundle hopping. At higher F ($eRF \gg k_B T$), the electric-field dependence of $\sigma(F)$ is not thermally activated and $\sigma \sim \exp[-(F_0/F)^{1/2}]$ for quasi-1D VRH where F_0 is a constant.

The thermoelectric power S in the 3D metallic states is proportional to T/E_F [$S(T) \propto T/E_F$]. However, in the localized states, the conduction is due to charge hopping and $S(T)$ is determined by[28,29]

$$S(T)=\frac{k_B}{2e}\frac{W^2}{k_B T}\left[\frac{d}{dE}\ln f(E)g(E)\mu(E)\right]_{E_F} \propto \frac{W^2}{T} , \tag{14}$$

where W is the range of energy contributing to the conduction, $f(E)$ is the distribution function, and $\mu(E)$ is the mobility. According to Mott and Davis,[29] W is assumed to be the hopping energy. For the interchain hopping in quasi-1D VRH, $W \sim k_B(T_0 T)^{1/2}$ (Ref. 28) and thus

$$S(T)_{\perp} \propto (T_0 T)/T \sim \text{const} , \tag{15}$$

and for the intrachain hopping, $W \sim k_B T_0 = \text{const}$ so that

$$S(T)_{\parallel} \propto 1/T . \tag{16}$$

The total thermopower is contributed by both interchain and intrachain hopping so that the T dependence is

$$S(T)=S_0+B/T , \tag{17}$$

where S_0 and B are only weakly T dependent.

The dielectric constant ϵ is a parameter sensitive to localization. In general $\epsilon \propto N(E_F)L^2$. If the metallic bundles are modeled by a rectangular box of side lengths L_i, we obtain a more accurate formula[32]

$$\epsilon_i=\epsilon_{i,\infty}+\frac{2^{9/2}}{\pi^3}e^2 N(E_F)L_i^2 , \tag{18}$$

where $\epsilon_{i,\infty}$ is from anisotropic core polarization. In principle, this formula can be applied at any temperature.

C. EPR properties of quasi-1D spin diffusion

EPR is a powerful probe of spin localization and dimensionality. One can get the information through the measurement of susceptibility, g factor, linewidth, and line shape. The EPR linewidth is determined by spin-spin relaxation time (T_2). There are several relaxation processes which cause the shortening of T_2 and hence the broadening of an EPR line. One of them is the spin-lattice relaxation, which shortens the lifetime of a spin state and broadens the line. The spin-lattice relaxation is characterized by a time T_1. If we, represent all the other relaxation processes by a time T_2', we can write $\Delta H_{1/2}$, the half linewidth of a Lorentzian line at half power, as[33]

$$\Delta H_{1/2}=\gamma^{-1}\frac{1}{T_2}=\gamma^{-1}\left[\frac{1}{T_2'}+\frac{1}{2T_1}\right] , \tag{19}$$

where $\gamma=ge/2mc \approx 1.7588\times 10^7$ (Hz/G) is the gyromagnetic ratio.

For an isolated spin, there are mainly two contributions to $1/T_2'$: spin dipole-dipole interaction $\omega_d=\gamma H_d$ where

$$H_d^2=5.1(g\mu_B n)^2 S(S+1) \tag{20}$$

and hyperfine interaction $\omega_h=\gamma H_h$ where

$$H_h=\tfrac{1}{3}A^2 I(I+1) . \tag{21}$$

Here g is the g factor, μ_B is the Bohr magneton, n is the spin concentration, A is the hyperfine constant, and I is the nuclear spin.[34] However, if the spin is movable or there exists exchange interaction $\omega_e=\gamma H_e$ between the spins, the lines will be narrowed (motional narrowing or exchange narrowing) such that[35]

$$1/T_2'=\frac{\frac{10}{3}\omega_d^2+\omega_h^2}{\omega_e} , \tag{22}$$

if $\omega_e \gg \omega_d, \omega_h$.

The EPR line shape due to dipole or hyperfine broadening is normally Gaussian. The spin motion or exchange will alter the EPR line shape. For a 3D motion or exchange, the line shape becomes close to Lorentzian shape, corresponding to an exponential decay of transverse magnetization with time t, $\Phi(t) \sim \exp(-\eta t)$; for a 1D spin motion, $\Phi(t) \sim \exp[-(\beta t)^{3/2}]$.[36] Here η and β are constants. For a quasi-1D spin motion, we have[36]

$$\begin{aligned}&\Phi(t)=\exp[-\phi(t)] ,\\ &\phi(t) \approx \frac{\langle\omega^2\rangle}{(J'/\hbar)^2}\Psi(t/t_c) ,\\ &\Psi(t/t_c)=\int_0^{t/t_c}[(t/t_c)-x]x^{-1/2}\\ &\qquad\qquad \times\exp(-4x^{3/2})I_0^2(2x^{3/2})dx ,\end{aligned} \tag{23}$$

where $\langle\omega^2\rangle$ is the second moment of an un-narrowed line, J' is the spin interchain coupling, I_0 is the modified zero-order Bessel function, and t_c^{-1} is the interchain hopping rate[36]

$$t_c^{-1} \approx (J'/J)^{1/3}J'/\hbar . \tag{24}$$

Here J is the spin in-chain coupling. The function $\Psi(y) \sim y^{3/2}$ when $y \ll 1$ and $\Psi(y) \sim y$ when $y \gg 1$. If the interchain coupling is weak, i.e., $(J'/\hbar)^2 \ll \langle\omega^2\rangle$, $\Phi(t)$ will decay very rapidly and become negligibly small by the time $t/t_c \sim 1$. In this case $\Phi(t) \sim \exp[-(\beta t)^{3/2}]$, resulting in a 1D spin-diffusion EPR line shape. On the other hand, if interchain coupling is significant, there is considerable contribution from long-time decay, i.e., when $t/t_c > 1$. Hence $\Phi(t) \sim \exp(-\eta t)$, resulting in a 3D spin diffusion EPR line shape. Figure 1 shows how the line shape depends on the ratio $R=(J'/\hbar)\langle\omega^2\rangle^{1/2}$.

It is noted that the above approach is based on the assumption $J/\hbar \gg \langle\omega^2\rangle^{1/2}$ so that in-chain motion is

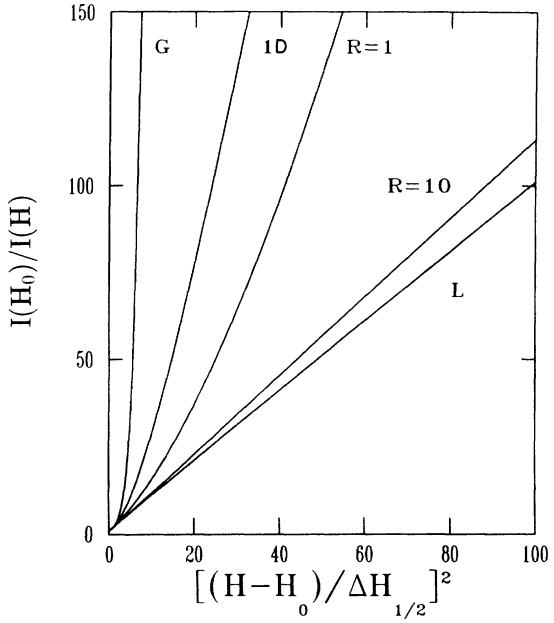

FIG. 1. Theoretical EPR line shapes for quasi-1D spin diffusion with $R=(J'/\hbar)\langle\omega^2\rangle^{1/2}=0$, 1, and 10. The 3D spin diffusion gives Lorentzian line shape (L) and localized spin gives Gaussian line shape (G).

coherent. Were it not satisfied, the EPR line shape would deviate from the Lorentzian line shape in the wings and approach a Gaussian distribution. Thus the depletion from Lorentzian line shape at wings may not necessarily indicate the quasi-one-dimensionality of spin diffusion.

III. EXPERIMENTAL METHODS AND RESULTS

The emeraldine base of polyaniline (PAN-EB) (Fig. 2) was prepared by chemical means[20] and cast into films from N-methly-2-pyrrolidinone.[37] The films are partially crystalline with coherence lengths up to a maximum of ~ 50 Å.[26] The crystalline percentage varies from a few to a few tens percent. The films were stretched up to $l/l_0=4$ through a uniaxial web stretching device where it contacts two heated rollers.[37] The stretching takes place at the first roller, which is set at 148 °C. Upon stretching, crystalline coherence length increases up to approximately as high as 100 Å in the longitudinal direction and

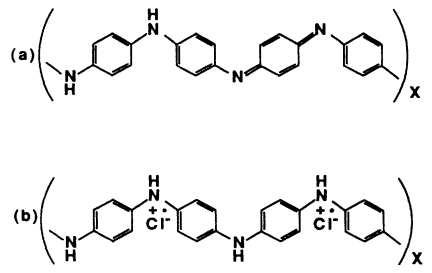

FIG. 2. Schematic structure of (a) emeraldine base form of polyaniline (PAN-EB), and (b) fully doped emeraldine salt form of polyaniline in the polaron lattice state (PAN-ES).

remains approximately the same in the transverse direction.[26] The crystalline percentage increases somewhat, varying from sample to sample up to 50%. The bulk density is about 1.0 g/cm^3 for unoriented PAN-EB films and 0.9 g/cm^3 for 1:4 stretched films, compared with 1.34 g/cm^3 obtained by flotation techniques. Note that this latter value is approximately the same as the calculated value from crystal structure. Thus the compactness of the films is roughly 0.7 ± 0.1 depending on the stretching ratios. The free-standing films were doped approximately to [Cl]/[N]$=0.12\pm0.05$, 0.37 ± 0.03, and 0.49 ± 0.02 by equilibrating with HCl solution of pH$=2.5$, 1.5, and 0.0, respectively, for 48 h (Ref. 38) and subsequently drying under dynamic vacuum for one day. The crystalline percentage slightly decreases and the coherence length shortens (20–25 Å) upon doping.[26]

A. dc conductivity

The four-probe conductivities $\sigma_{dc}(T)$ for 1:4 stretched samples at different doping levels are plotted in Fig. 3. The room-temperature values of σ are sensitive to the moisture concentration and can vary by a factor of 5–10. The highest σ value for 1:4 stretched samples (unpumped) is 400 S/cm. The temperature dependence of $\sigma(T)$,

$$\sigma_{dc}(T)\propto\exp[-(T_0/T)^{1/2}]\ , \tag{25}$$

is the best fit to the data for samples at all of the doping levels. We can easily distinguish the exponent $\frac{1}{2}$ from $\frac{1}{3}$ or $\frac{1}{4}$ using σ_{dc} data within the temperature range of the experiment (30–300 K). The values of T_0 decrease as the doping levels increase and are slightly different for paral-

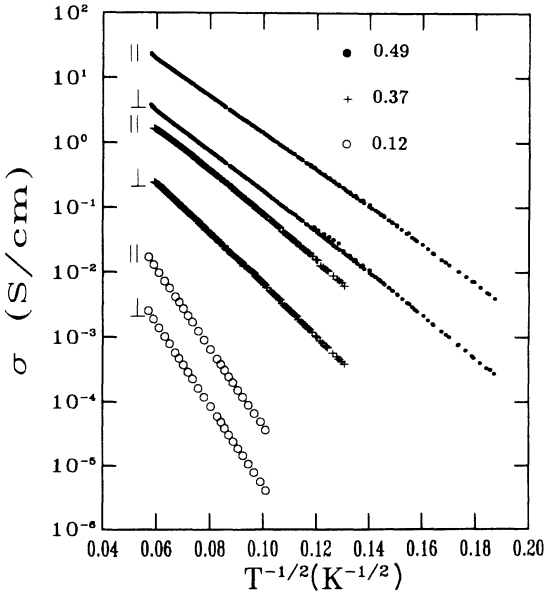

FIG. 3. Temperature dependence of dc conductivity of $x=$[Cl]/[N] 0.12 (○), 0.37 (+), and 0.50 (●) doped 1:4 stretched PAN-ES (HCl) films in the directions parallel and perpendicular to the stretching axis. The samples have been pumped overnight before the experiments.

lel and perpendicular directions at the same doping levels (Fig. 3). They decrease with increasing moisture concentration.[27] The values of T_0 for vacuum-dried samples are listed in Table I.

B. Thermoelectric power

The thermopower was measured using a modification of the technique of Chaiken and Kwak,[28,39] in which a temperature difference of typically no more than 1 K is applied across the sample. In general the dc conductivities, thermopower, and electric-field-dependent conductivity were measured on the same sample bath.

The thermoelectric power $S(T)$ of PAN-ES ($x \approx 0.50$) for different stretching ratios (1:4, 1:3, and 1:1) is shown in Fig. 4. All the data show aspects of a "U-shaped" or partially U-shaped T dependence. This feature is preserved for all the polyaniline derivatives as well. In Fig. 5 we compare $S(T)$ of unoriented PAN-ES with that of the derivative POT-ES [poly(*o*-toluidine) salt][28] and SPAN (sulfonated polyaniline).[40] These U-shaped curves show different shifts in the y axis, reflecting a constant contribution to $S(T)$ for all the polymers. Though it varies for different polymers and different stretching ratios, this constant contribution (represented by S_0) is always more *negative* for $S_\perp$, the *transverse* component of $S(T)$, compared with that of $S_\parallel$, the *parallel* component of $S(T)$.

At high temperatures, $S(T)$ of PAN-ES is approximately proportional to T, i.e., $S(T)=CT$ except for the additional constant S_0. Note that S_0 is *negative* for all samples. The proportionality coefficient C is positive and *independent* of orientation and stretching ratios of samples. This feature reveals itself more rigorously at lower doping levels as shown in Figs. 6 and 7. We can see that $S(T)=CT$ and C is essentially the same for both parallel and perpendicular directions. However C is *increased* as doping levels *decrease,* as shown in Figs. 4, 6, and 7. For one of the derivatives of polyaniline, poly(2-ethoxyaniline) (PEA-ES), the slope increases with increase of stretching in contrast to the behavior of PAN-ES.[41]

At lower temperatures, the relation $S(T)=S_0+B/T$ is followed by all of the samples. In Fig. 8 the values of $S(T)$ for both POT-ES and SPAN are replotted versus $1/T$. From Fig. 8 we can see that B is *positive* and S_0 is *negative* as is mentioned previously.

The minimum of the U-shaped curve occurs at different temperatures for different samples. For PAN-ES, it occurs below 100 K for $S_\parallel$ and between 100 and 200 K for $S_\perp$, depending on the degree of orientation. For polyaniline's derivatives, it often takes place between 250 and 300 K.

The T dependence of S is then expressed approximately as

TABLE I. Dependence of T_0 (K) on doping levels for conductivity parallel and perpendicular to the stretching direction.

Doping	0.12	0.37	0.49
$T_0,\parallel$	19 000	6000	4300
$T_0,\perp$	21 400	8300	5200

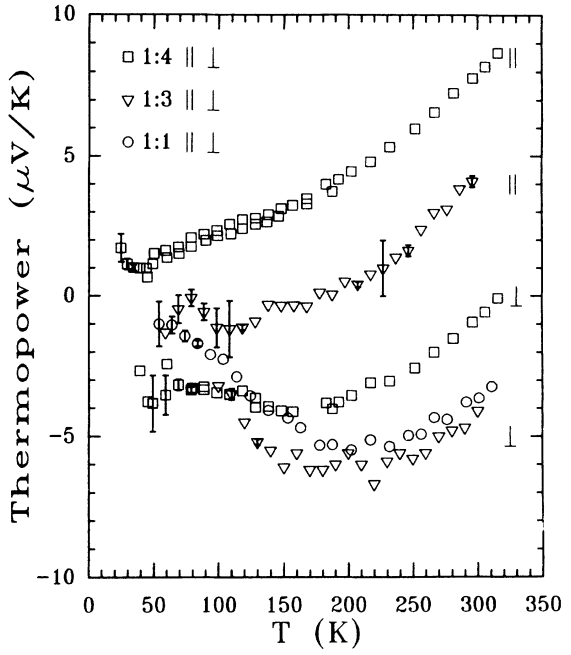

FIG. 4. Comparison of temperature dependence of thermoelectric power of PAN-ES ($x=0.50$) at stretching ratios 1:4 (□), 1:3 (▽), and 1:1 (○).

$$S(T)=S_0+B/T+CT\ , \tag{26}$$

with S_0, B, and C only weakly T dependent. Though this formula represents a general feature of $S(T)$, we found that the transition from $S(T)\propto T$ to $S(T)\propto 1/T$ is sharper than the simple summation of the two terms.

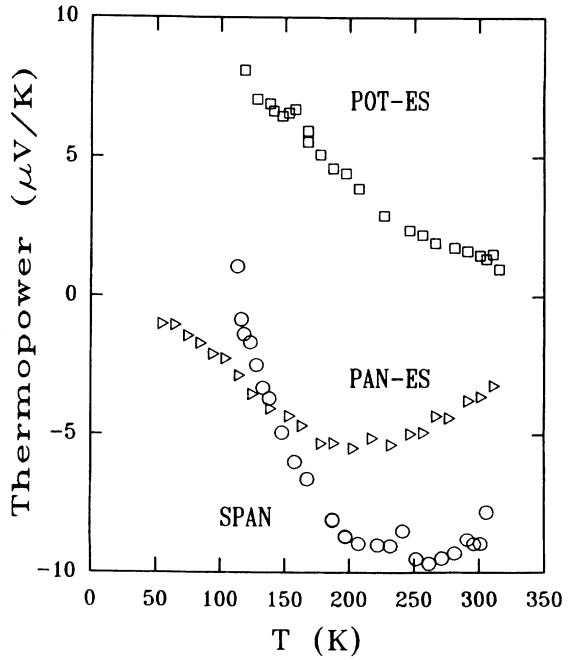

FIG. 5. Thermoelectric power of PAN-ES ($x=0.50$) (▷), POT-ES ($x=0.50$) (□), and SPAN (○). All the samples are unoriented.

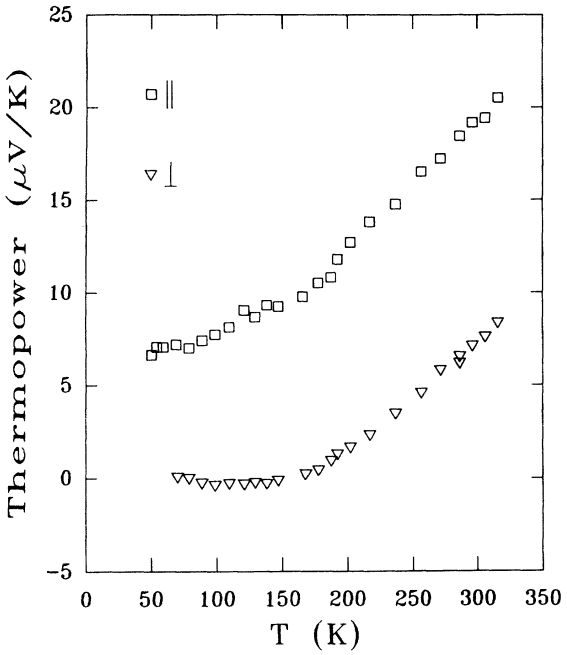

FIG. 6. Thermoelectric power of PAN-ES at $x=0.37$ doping level. Sample is 1:4 stretched.

C. Microwave dielectric constant

A cavity perturbation technique is used for the microwave dielectric constant ϵ and conductivity σ_{mw} measurement.[42,43] The values of ϵ and σ_{mw} can be obtained by measuring the sample induced-cavity resonance frequency shift $\delta=(f-f_0)/f_0$ and loss $\Delta=(F-F_0)/F_0$ where f and F (f_0 and F_0) are resonance frequency and linewidth at half power with (without) a sample. The ϵ and σ_{mw} can then be evaluated such that

$$\epsilon'-1=1/N\frac{\delta(\alpha/N-\delta)-(\Delta/2)^2}{(\Delta/2)^2+(\alpha/N-\delta)^2}\,,$$
$$\epsilon''=\alpha/N^2\frac{\Delta/2}{(\Delta/2)^2+(\alpha/N-\delta)^2}\,, \tag{27}$$

and $\sigma_{mw}=\omega\epsilon_0\epsilon''$ (ω is the angular frequency and ϵ_0 is the vacuum dielectric constant) where α is the filling factor and N is the depolarization factor.[42,43]

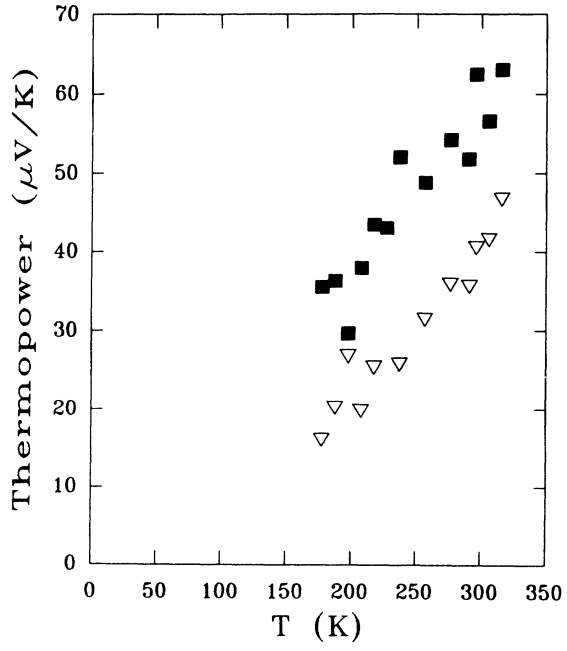

FIG. 7. Thermoelectric power of PAN-ES at $x=0.12$ doping level. Sample is 1:3 stretched.

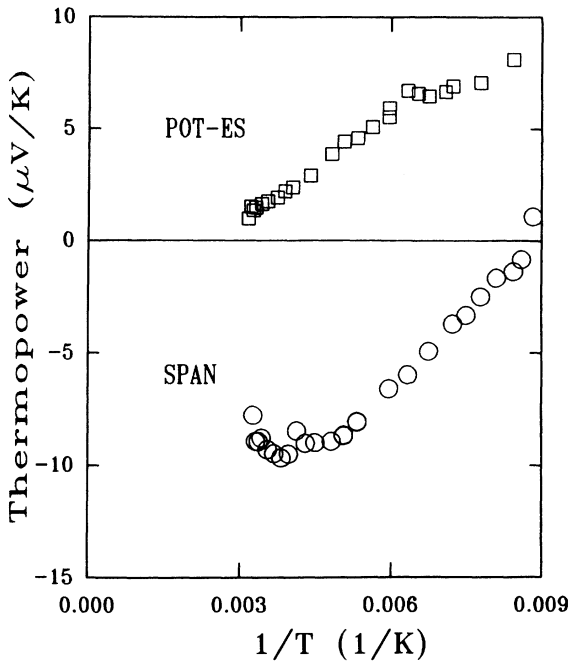

FIG. 8. Thermoelectric power of POT-ES ($x=0.50$) (□) and SPAN (○) doping as function of $1/T$ where T is the temperature.

The values of ϵ at the zero-temperature limit for $x=0.50$-doped PAN-ES with different stretching ratios are shown in Fig. 9. The error bars account for uncertainties in geometric factors and compactness of the samples. The values of $\epsilon_\parallel$ (parallel component of ϵ) increase significantly with stretching ratios. For 1:4 stretched samples, anomalously large $\epsilon_\parallel$ ($\sim 1500\pm500$ at 295 K and $\sim 100\pm10$ at $T\rightarrow 0$) was obtained (Fig. 10). However, the low-temperature values of $\epsilon_\perp$ (perpendicular component of ϵ) are approximately equal to 26, *independent* of stretching ratios within the experimental uncertainties.

Both $\epsilon_\parallel$ and $\epsilon_\perp$ increase with temperature as shown in Fig. 10. The temperature dependence of ϵ is approximately represented by

$$\epsilon(T)\approx\epsilon(0)+KT^2\,, \tag{28}$$

where the coefficient $K_\parallel\approx 1.4\times10^{-2}(K^{-2})$ for $\epsilon_\parallel$ and $K_\perp\approx 2.0\times10^{-3}(K^{-2})$ for $\epsilon_\perp$.

D. Electric-field dependence of conductivity

A high electric field is applied to the samples by a pulse generator with a maximum voltage of 100 V. Both two-

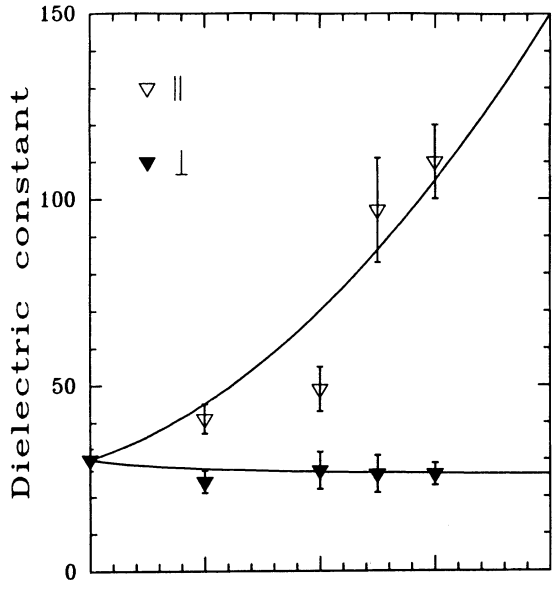

FIG. 9. The comparison of $\epsilon(T\rightarrow 0)$ at different stretching ratios. The solid lines represent $\epsilon_{\|}=\epsilon_{3D}+\xi(l/l_0)^2$ and $\epsilon_{\perp}=\epsilon_{3D}+\xi(l_0/l)$, where ξ is a constant.

probe and four-probe techniques are used in the measurements.[44] In the two-probe measurement, a sandwich configuration is adopted. The typical electric-field dependence of PAN-ES is shown in Fig. 11. The film has a thickness of 20 μm and, hence, the electric field is as high as 10^4 V/cm. We can see that the electric-field dependence of conductivity roughly follows Eq. (12) and *R increases* with a *decrease* of the temperature.

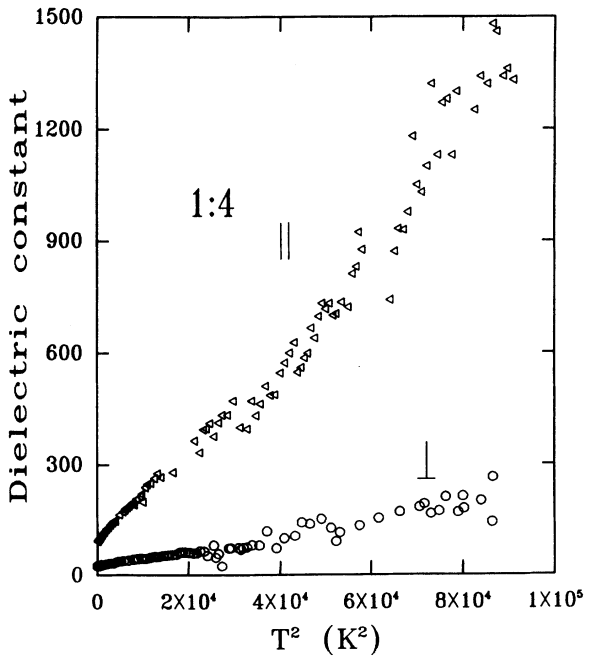

FIG. 10. Temperature dependence of the dielectric constant for a 1:4 stretched sample in the electric field F parallel (◁) and perpendicular (○) to the stretching direction. Sample is doped to $x=0.50$.

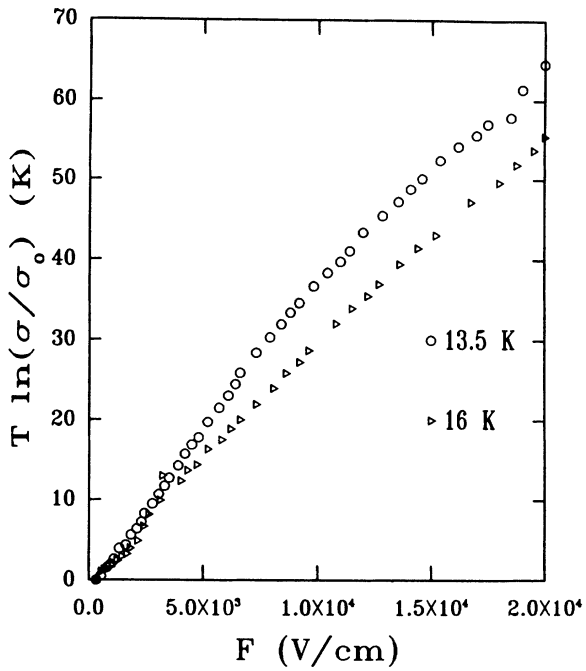

FIG. 11. Electric-field dependence of conductivity $\sigma(F)$ at temperature 13.5 K (○) and 16 K (▷) by two-probe technique. A sandwich configuration is used and the field is perpendicular to the plane. The sample is 1:4 stretched PAN-ES at $x=0.50$ doping level.

Since contact resistance and space-charge limited injection may play a role in $\sigma(F)$ in the two-probe measurement, we also employed a 4-probe technique. In this case two gold electrodes were coated on both sides of the samples with a narrow gap in between. The current was applied through the two electrodes on one side and voltage was measured between the two electrode on other side. The results for 1:4 stretched samples are plotted in Fig. 12. *The relation Eq. (12) still holds.* When the electric field is in parallel to the stretching direction, the electric-field dependence of σ is stronger than that for the perpendicular direction, i.e., $R_{\|}>R_{\perp}$. At 25 K, we obtain $R_{\|}=110$ Å and $R_{\perp}=20$ Å by fitting the data to Eq. (12).

E. Electron paramagnetic resonance

Electron paramagnetic resonance (EPR) has been performed on unoriented PAN-ES. The EPR peak-to-peak linewidth ΔH_{pp} varies from 0.29 to 0.6 G at room temperature, depending on oxygen concentration. Its T dependence is presented[45] in Fig. 13. At high temperatures ($T>100$–200 K), $\Delta H_{pp}\propto T$. At low temperatures, however, ΔH_{pp} increases while T decreases. A minimum occurs between 100 and 200 K, depending on the oxygen concentration. There is a sudden decrease of ΔH_{pp} at ~ 10 K. However, this drop, though it occurs quite often, is not reproducible.

The spin-lattice relaxation time T_1 is measured by saturation methods. Assuming homogeneous broadening with an EPR line shape $I(\nu)$ [$\int I(f)df=1$], the EPR absorption signal Y (single integral) is given by[46]

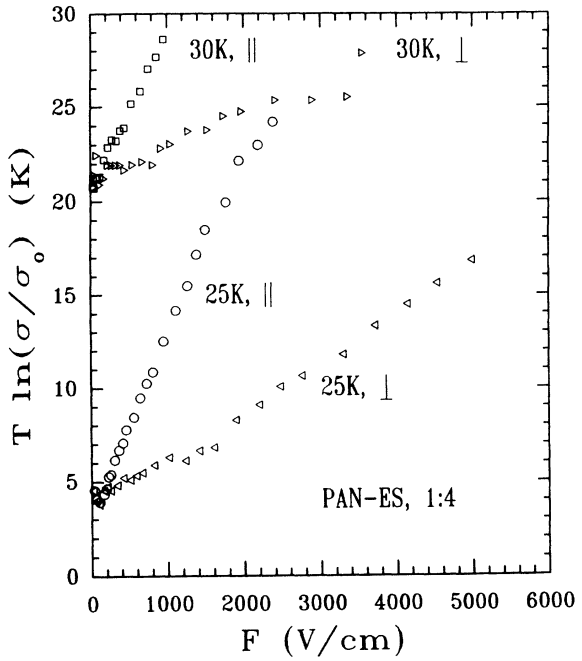

FIG. 12. Electric-field dependence of conductivity $\sigma(F)$ at temperature 25 K (○) and 30 K (▷) by four-probe technique. A planar configuration is utilized. The sample is 1:4 stretched PAN-ES at $x=0.50$ doping level.

$$Y \propto \frac{H_1}{1+\frac{1}{2}\gamma^2 H_1^2 T_1 I(f)} ,$$
$$\frac{H_1}{Y} \propto 1+\tfrac{1}{2}\gamma^2 T_1 I(f) H_1^2 . \tag{29}$$

Thus, we expect to obtain a linear plot of H_1/Y vs H_1^2 where $H_1=KP^{1/2}$ and P is the microwave power. The coefficient K is obtained by measuring the microwave frequency shift ($f_0 \rightarrow f$) induced by a metallic sphere with radius a according to[47]

$$H_1^2 = \left[\frac{f^2-f_0^2}{f_0^2}\frac{10}{\pi\Delta\nu a^3}\right]P = 0.628P , \tag{30}$$

where mks units are used except for H_1 (in G) and $\Delta\nu$ is unloaded full half-power width of the EPR cavity.

The EPR saturation results for one sample with ΔH_{pp} (295 K)=0.58 G is shown in Fig. 14. The linear relation indicates that EPR line broadening is homogeneous. From the slope we obtain $T_1(295\text{ K})=0.98\times10^{-7}$ sec and $T_1(10\text{ K})=2.2\times10^{-7}$ sec.

The EPR low-temperature line shapes of PAN-ES and of POT-ES are analyzed in Fig. 15. Here the y axis is the reciprocal intensity (single integral of EPR derivative signal) normalized to its central value and the x axis is the square of the static magnetic field measured from the center of the EPR line and normalized to the half-power linewidth. It is seen that the line shape of PAN-ES is very close to a Lorentzian shape while that of POT-ES is close to a 1D line shape.

IV. DISCUSSION

The temperature and electric-field dependence of conductivity (Figs. 3, 11, and 12) suggest that the quasi-1D VRH model[28-30] may be a proper model for charge conduction. The relation $\sigma(T)\sim\exp[-(T_0/T)^{1/2}]$ suggests the relevance of three models: quasi-1D variable-range hopping between the nearest-neighboring chains,[28,30]

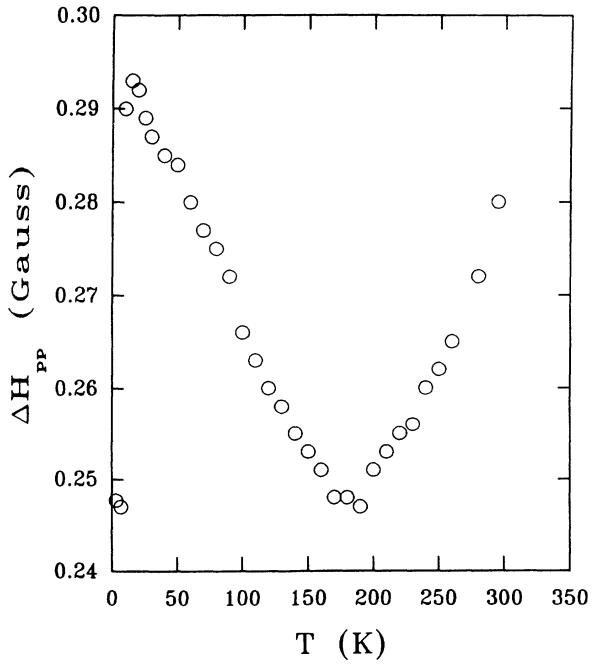

FIG. 13. EPR peak-to-peak linewidth of unoriented PAN-ES ($x=0.50$) as a function of temperature [P. Vaca *et al.* (unpublished)].

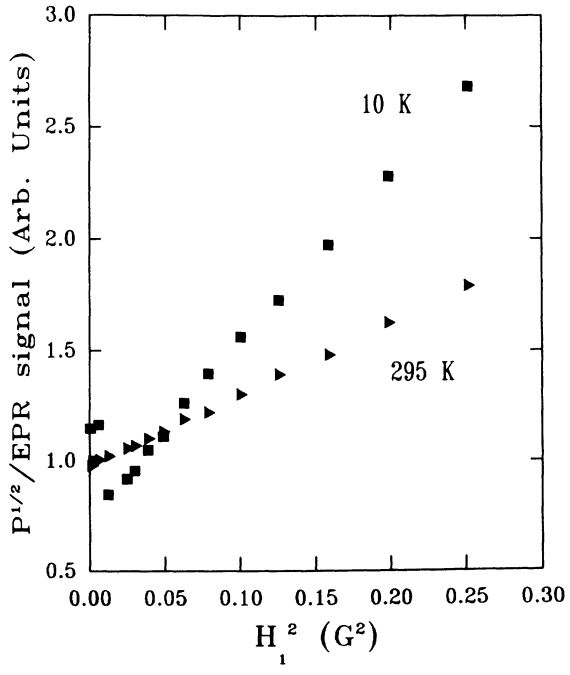

FIG. 14. The saturation dependence of the EPR signals at 10 and 295 K for unoriented PAN-ES ($x=0.50$). The slope is proportional to T_1.

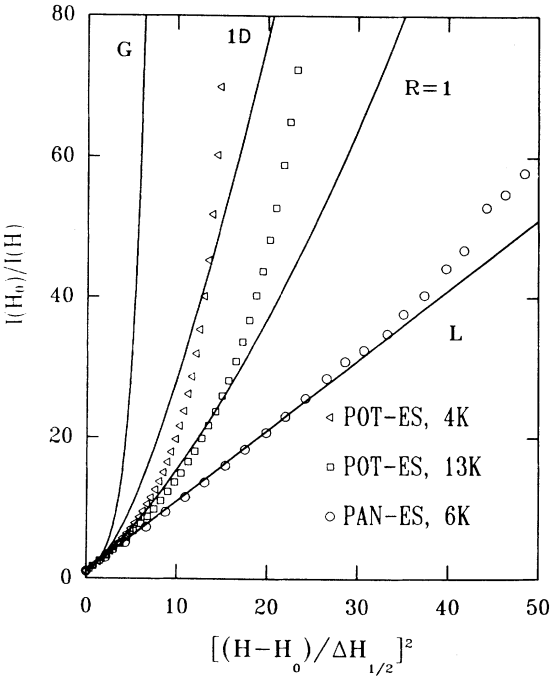

FIG. 15. Analysis of EPR line shapes of PAN-ES and POT-ES at low temperatures in comparison with theoretical line shapes for quasi-1D diffusion.

hopping in granular metals,[22,48] and 3D VRH with the presence of a Coulomb gap at Fermi level.[49] The last model is unlikely to be relevant due to the presence of finite density states at Fermi energy[28,50] and the T-dependent thermopower.[28] The electric-field dependence $\sigma(F) \propto \exp(-eRF/k_BT)$ favors the quasi-1D VRH model [Eq. (12)]; granular metal systems show the electric-field dependence $\sigma(F) \propto \exp(-F_0/F)$.[48] From $T_0 = 5000$ K and $N(E_F) = 1.6$ states per eV per 2 rings,[50] we estimate $L_\parallel = 50$ Å. This is similar to crystalline coherence length,[26] indicating that electrons are delocalized within the crystalline regions. From Eq. (12) we estimate a hopping distance $R_\parallel = 110$ Å at 25 K. This is self-consistent with the most probable hopping distance from Eq. (13) where $R = (L_\parallel/4)(T_0/T)^{1/2} = 130$ Å, supporting quasi-1D VRH as a proper model for charge conduction. The transverse $\sigma(F)$ data give $R_\perp = 20$ Å. This value is much larger than the interchain separation (3.5–5 Å), probably due to the contribution from misaligned chains. It may also suggest that the effective 1D unit is not a single polymer chain but a bundle of polymer chains with effective transverse dimension on the order of 20 Å.

The thermopower data (Figs. 4–7) support the above analyses and further suggest that there exist *three-dimensional* metallic regions in the samples. First we note that thermopower data of PAN-ES and its derivative [POT-ES (Ref. 28)] and SPAN (Ref. 40)] are similar (Fig. 5) and that the relation $S(T) = S_0 + B/T$ is followed by the polyaniline's derivatives, where S_0 is always *negative* and B/T is always *positive*[28,40] (Fig. 8). This behavior is in accordance with quasi-1D VRH [Eq. (17)]. The similarity of $S(T)$ between PAN-ES and its derivatives leads us to apply the expression $S(T) = S_0 + B/T$ to the thermopower of PAN-ES at low temperatures. Although the temperature range is too small for this application to be unambiguous, this is supported by the following consideration. Since $S_0 < 0$ and $B/T > 0$ are contributions from interchain and intrachain VRH, respectively [Eqs. (15) and (16)], it is expected that $S_\perp$ is *more negative* than $S_\parallel$, as confirmed by the experiment (Fig. 4). Also, it is noted that $S_\perp$ should not contain a $1/T$ term which is due to the intrachain quasi-1D VRH. Thus, one expects that the $1/T$ contribution to $S_\perp$ at low T should decrease as the degree of orientation increases. This is in accordance with a comparison of $S(T)_\perp$ of 1:3 and 1:4 stretched polymers (Fig. 4). For the higher temperatures, $S(T) \propto T$ except for a constant. This constant component indicates interchain hopping still plays a role in the conduction. It is well known that $S(T) \propto T/E_F$ for free electrons. For the high-T regime, since the linear T dependence is *independent* of orientation, we propose that this is due to the contribution of nearly-free-electrons transporting in 3D "metallic" regions of the polymer. The decrease of the linear slope of $S(T)$ vs T with the doping level may reflect effective medium effects[54] as well as the change in the PAN-ES unit cell with doping affecting the E_F and 1D localization length. In contrast to PAN-ES, the slope of oriented PEA-ES strongly depends on the orientation degree, a signature of one dimensionality. In summary, $S(T)$ can be decomposed into three components: a negative constant due to interchain quasi-1D VRH, a positive component $\propto 1/T$ due to intrachain 1D VRH, and a positive component $\propto T$ due to free charge carriers in 3D "metallic" regions. The first two components are likely contributed from amorphous regions.

The dielectric constant data support the existence of these 3D metallic regions. It is noted that giant dielectric constants were also observed in many TCNQ salts[4] (along the highly conducting axis) and $IrCl_6$-doped polyacetylene.[51] The major difference between PAN-ES and TCNQ salts is that PAN-ES has a much larger transverse dielectric constant $\epsilon_\perp$ (≈ 26; see Fig. 9) at low T (for TTF-TCNQ, $\epsilon_\perp = 6$). Since $\epsilon_\perp$ is independent of stretching ratio, it is unlikely to be due to the contribution of misaligned chains. Also, the mosaic spread of 1:4 stretched polymer chains is $\pm 7°$ for crystalline regions,[26] too small to account for the observed $\epsilon_\perp$. We thus suggest that $\epsilon_\perp$ is mainly due to the transverse polarization of electrons. Four origins were proposed for large $\epsilon_\parallel$ in TCNQ salts: pinned charge-density-wave (CDW) states,[52] small single electron bandgaps,[4] (quasi-1D) conductors with large localization lengths,[3,53] and the presence of mobile charge bipolarons.[55] The T dependence of σ, the susceptibility,[50,56] and the optical absorption spectra[57] do not support the existence of band gaps, CDW, or mobile bipolaron states in PAN-ES. Assuming that the large $\epsilon_\parallel$ is the signature of a conductor with large localization lengths, the relatively large $\epsilon_\perp$ in PAN-ES supports the fact that the electron wave functions extend beyond a single chain, since $\epsilon \propto L^2$ [see Eq. (18)]. To estimate L quantitatively, Eq. (18) is used. The core polarization contributions ϵ_∞ are estimated from PAN-EB. For 1:4 stretched PAN-EB, $\epsilon_\parallel = 10$ and $\epsilon_\perp = 4$. Hence, we obtain

$L_{\parallel}=40$ Å for 1:4 stretched PAN-ES using $\epsilon_{\parallel}-\epsilon_{\infty}\approx 100$ and $L_{\perp}=20$ Å for $\epsilon_{\perp}-\epsilon_{\infty}\sim 22$. Since the value 20 Å is much larger than the interchain separation of polymer chains [3.5 Å (Ref. 26)], it is confirmed that the conduction electrons are delocalized transversely beyond a single conducting chain. In contrast, the $\epsilon_{\perp}$ of TTF-TCNQ at low T is 6 (Ref. 4) and POT-ES has $\epsilon_{\perp}=7$.[28] In these materials the contribution of conduction electron to $\epsilon_{\perp}$ is small ($\epsilon_{\perp}$ is mainly from the core polarization), apparently due to the limitation of electrons to single conducting chains. We thus consider PAN-ES as a quasi-1D conductor consisting of bundles of N coupled parallel chains. This result is consistent with $S(T)$ at higher ($T>100$ K) where 3D metallic behavior was observed (Figs. 4–6). Since the estimated sizes of the "metallic" bundles are similar to the crystalline coherence length of crystalline regions, it is likely that these "metallic" bundles are the crystalline regions of the polymers. It is noted that the values of L are underestimated since the measured ϵ is an average of ϵ from the crystalline and the amorphous regions. Due to the strong localization of electron wave functions in the amorphous regions (hence small ϵ) the averaged ϵ is expected to be smaller than that in crystalline regions.

The temperature dependence of $\epsilon(T)\propto T^2$ probably results from a temperature-dependent localization length. We assume the electrons are trapped in a well (metallic bundles) surrounded by a disorder potential $V(x)$. To the first-order approximation, $V(x)\approx V_0+V'x$ where x is the distance into disordered regions from the metallic regions and V' is the rate of change of V with respect to x. The localization length is determined by

$$L(T)=\frac{\int x\exp[-V(x)/k_BT]}{\int \exp[-V(x)/k_BT]}=\frac{k_BT}{V'}\ . \tag{31}$$

Hence $\epsilon(T)\propto L(T)^2\propto T^2$.

The conduction electrons in the amorphous regions are expected to be localized to single chains. The amorphous regions likely give rise to the Curie spins observed in EPR. From the EPR linewidth at low temperatures we may estimate the exchange or diffusive rate of these spins. According to Eq. (20), and using $n\sim 2\times 10^{20}$ (cm^{-3}),[50] we obtain $H_d^2\sim 60$ G^2. The hyperfine constant of amine nitrogen NH^+ is 30 G (Ref. 33) and thus $H_h^2\sim 600$ G^2 [see Eq. (21)]. Assuming the linewidth $\Delta H_{1/2}(T\rightarrow 0)=0.2$ G (from the low-temperature data) and Eq. (22) (the contribution from T_1 is negligible), we obtain $H_e\sim 4000$ G or exchange (diffusive) rate $\sim 7\times 10^{10}$ Hz. This rate is much smaller than the scattering rate ($1/\tau\sim v_F/l_i\sim 10^{15}$ Hz). Therefore, in the amorphous regions electrons are in the localized regime and hopping conduction is expected.

To summarize the previous discussions, PAN-ES is a heterogeneous quasi-1D DS composed of 3D "metallic" crystalline regions and 1D localized amorphous regions. Due to the crystalline order, interchain transfer $w>w_c$ in the crystalline regions and 3D "metallic" bundles are formed. These regions give rise to $S(T)\propto T$, *independent of orientation.* In the amorphous regions, the disorder reduces the interchain transfer rate so that $w<w_c$. Thus, electrons are localized to a single chain and hopping is the dominating conduction mechanism. The electron hopping gives rise to $S(T)=S_0$ (interchain quasi-1D VRH) and $S(T)\propto 1/T$ (intrachain quasi-1D VRH). Macroscopic σ is dominated by the most difficult transport component, that is, the interchain hopping in the amorphous regions. It is possible that the observed $\sigma(T)$ is due to interbundle hopping since the observed transverse hopping range $R_{\perp}\sim 20$ Å is the same as the bundle size. However, as we pointed out before, the misaligned chains may play a role as well.

The origin of the formation of the "metallic" bundles in PAN-ES is attributed to the significant interchain coupling and coherence in the crystalline regions. We can see this by comparison of PAN-ES and its nonmetallic derivative POT-ES. PAN-ES has Lorentzian line shape, suggesting $J'/\hbar\gg\langle\omega^2\rangle^{1/2}$ (Fig. 15). However, POT-ES has a line shape closer to those of 1D spin diffusion such that $J'/\hbar\sim\langle\omega^2\rangle^{1/2}$. The reduced J' or interchain transfer rate $\omega\sim t_0^{-1}$ [see Eq. (24)] is caused by the reduction of the interchain coupling and interchain coherence in POT-ES.[28] Hence, even within the crystalline regions the condition $\omega>1/2\tau$ may not be fulfilled for POT-ES so that the electron states are still in the 1D localized regime.

The difference of PAN-ES and its derivatives in electron localization can be understood in terms of dimensionality of electron states. The metallic bundles in PAN-ES are similar to 3D thin metallic wires where Thouless localization plays important roles. Given the magnitude of disorder, Thouless localization is much weaker than Mott's 1D localization. The difference of Thouless localization and Mott's 1D localization may be the origin of the difference in electron localization of PAN-ES and its derivatives.

The 3D character of the "metallic" states in conducting polymers may stabilize the "metallic" states against the Peierls instability. It is shown that when interchain coupling is comparable with the Peierls gap, Peierls instability is suppressed.[1] As we know, Peierls ground states exist in many undoped polymers. The doping processes likely increase the interchain coupling and eventually suppresses the Peierls instability. On the contrary, TCNQ charge-transfer salts have much weaker interchain coupling so that the electron states are still 1D states and the Peierls instability plays an essential role at low temperatures.

One remaining question is the nature of a transition taking place between 100 and 200 K. The temperature dependence of thermopower changes from $S(T)\propto T$ at high temperatures to $S(T)\propto 1/T$ at low temperatures. The temperature of this transition $T_c\sim 100$–200 K. A similar change takes place for the T dependence of EPR $\Delta H_{pp}(T)$ (Fig. 12) in this temperature range. From the measured $T_1(295\text{ K})=0.98\times 10^{-7}$ sec for a sample with $\Delta H_{pp}=0.58$ G, we calculate the contribution of T_1 to the EPR linewidth at 295 K utilizing Eq. (19). We obtain $\Delta H_{1/2}=0.25$ G corresponding to $\Delta H_{pp}=0.29$ G. This value is in good agreement with the experimentally measured ΔH_{pp}, suggesting that EPR linewidth at high tem-

peratures is dominated by spin-lattice relaxation; motional narrowing causes $1/T_2'$ to be negligible. The linear T dependence of $\Delta H_{pp}(T)$ is thus due to $1/T_1 \propto T$ for direct process involving single-phonon absorption. As temperature decreases below T_c, the EPR linewidth starts to increase, suggesting the start of spin localization and, hence, the reduction of motional narrowing. This same localization process also changes $S(T)$ from metallic $[S(T) \propto T]$ at high T to localized $[S(T) \propto 1/T]$ at low T. Therefore, this transition, reflected in both $S(T)$ and ΔH_{pp}, is probably a localization-delocalization transition within the metallic bundles.

V. CONCLUSION

The electron states of PAN-ES are three-dimensional metallic states in the ordered crystalline regions. PAN-ES represents a class of quasi-1D disordered conductors which consist of bundles of well-coupled chains instead of isolated chains as in the conventional quasi-1D conductors. Within these bundles, the electrons are three dimensionally delocalized. These 3D metallic bundles are responsible for the large transverse dielectric constant, linear temperature dependence of thermopower, and its *independence* of orientation. From $\epsilon_\perp = 26$, we obtain a transverse localization length 20 Å. The longitudinal localization length is obtained, $L_\parallel \sim 40-50$ Å, independently from $\sigma_{dc}(T)$ and $\epsilon_\parallel(T \to 0)$. The bundles of PAN-ES can be compared to thin metallic wires where Thouless localization plays an important role. These metallic bundles are surrounded by amorphous regions in which the interchain hopping dominates the conductivity.

The formation of the metallic wires in PAN-ES is attributed to the significant interchain transfer rate in the ordered crystalline regions, which avoids 1D localization. However, in the amorphous regions the interchain transfer rate is suppressed by disorder so that electrons are still localized in essentially isolated chains. In contrast, the polyaniline derivatives, in which interchain coupling and coherence are suppressed due to the presence of side groups, are nonmetallic even within the crystalline regions.

Our results suggest an important role played by interchain coupling and three dimensionality in stabilizing the metallic states against the Peierls instability, as well as avoiding 1D electron localization in conducting polymers. Increasing the interchain couplings of the polymer is a critical strategy in improving conductivities and forming true metallic polymers.

ACKNOWLEDGMENTS

We are indebted to C. Li for kindly supplying us with transport results and Dr. P. Vaca for EPR linewidth results. Many thanks to K. R. Cromack and J. Yue for assistance. We also wish to thank Professor D. Stroud and Dr. M. J. Rice for discussions. This work was supported in part by the Defense Advanced Research Projects Agency through a grant monitored by the U.S. Office of Naval Research.

*Present address: Department of Physics, Room 13-3025, Massachusetts Institute of Technology, Cambridge, MA 02139.

[1]D. Jerome and H. J. Schulz, Adv. Phys. **31**, 299 (1982); *Highly Conducting Quasi-one-dimensional Organic Crystals,* Vol. 27 of *Semiconductors and Semimetals,* edited by E. M. Conwell (Springer-Verlag, Berlin, 1988).

[2]L. E. Shchegolev, Phys. Status Solidi A **12**, 9 (1972).

[3]A. A. Gogolin, Phys. Rep. **1**, 1 (1982); **5**, 269 (1988).

[4]S. K. Khanna, E. Ehrenfreund, A. F. Garito, and A. J. Heeger, Phys. Rev. B **10**, 2205 (1974).

[5]J. F. Kwak, P. M. Chaikin, A. A. Russel, A. F. Garito, and A. J. Heeger, Solid State Commun. **16**, 729 (1975).

[6]D. Kuse and H. R. Zeller, Phys. Rev. Lett. **27**, 1060 (1971).

[7]A. J. Heeger, S. A. Kivelson, J. R. Schrieffer, and W. P. Su, Rev. Mod. Phys. **60**, 781 (1988).

[8]N. Basescu, Z. X. Liu, D. Moses, A. J. Heeger, H. Naarmann, and N. Theophilou, Nature **327**, 403 (1987); T. Schimmel, W. Reiss, J. Gimeiner, G. Denninger, M. Schwoerer, H. Naarmann, and N. Theophilou, Solid State Commun. **65**, 1311 (1988); N. Theophilou, D. B. Swanson, A. G. MacDiarmid, A. Chakraborty, H. H. S. Javadi, R. P. McCall, S. P. Treat, F. Zuo, and A. J. Epstein, Synth. Met. **28**, D35 (1989).

[9]G. Leising, Phys. Rev. B **38**, 10313 (1988); H. S. Woo, D. B. Tanner, N. Theophilou, and A. G. MacDiarmid, Synth. Met. **41**, 159 (1991).

[10]H. H. S. Javadi, A. Chakraborty, C. Li, N. Theophilou, D. B. Swanson, A. G. MacDiarmid, and A. J. Epstein, Phys. Rev. B **43**, 2183 (1991); Y. Nogami, H. Kaneko, H. Ito, T. Ishiguro, T. Sasaki, N. Toyota, A. Takahashi, and J. Tsukamoto, *ibid.* **43**, 11 829 (1991).

[11]S. A. Kivelson and A. J. Heeger, Phys. Rev. Lett. **55**, 308 (1985); E. J. Mele and M. J. Rice, Phys. Rev. B **23**, 5397 (1981); D. S. Galvao, D. A. dos Santos, B. Laks, C. P. de Melo, and M. J. Caldas, Phys. Rev. Lett. **63**, 786 (1989); H.-L. Wu and P. Phillips, *ibid.* **66**, 1366 (1991); P. Phillips and H.-L. Wu, Science **252**, 1805 (1991).

[12]E. M. Conwell, H. A. Mizes, and S. Jevadev, Phys. Rev. B **40**, 1630 (1989); R. H. Baughman and L. W. Shacklette, *ibid.* **39**, 5872 (1989); L. W. Shacklette and R. H. Baughman, Mol. Cryst. Liq. Cryst. **189**, 193 (1990).

[13]Y. A. Firsov, in *Localization and Metal Insulator Transition,* edited by H. Fritzsche and D. Adler (Plenum, New York, 1985), p. 471; V. N. Prigodin, Y. A. Firsov, and W. Weller, Solid State Commun. **59**, 729 (1986); W. Apel and T. M. Rice, J. Phys. C **16**, L1151 (1983).

[14]J. Tsukamoto, A. Takahashi, and K. Kawasaki, Jpn. J. Appl. Phys. **29**, 125 (1990).

[15]G. Thummes, F. Korner, and J. Kotzler, Solid State Commun. **30**, 395 (1989).

[16]S. A. Kivelson and A. J. Heeger, Synth. Met. **22**, 371 (1988).

[17]A. B. Kaiser and S. C. Graham, Synth. Met. **36**, 367 (1990).

[18]Y. W. Park, C. O. Yoon, C. H. Lee, H. Shirakawa, Y. Suezaki, and K. Akagi, Synth. Met. **28**, D27 (1988).

[19]Z. H. Wang, C. Li, E. M. Scherr, A. G. MacDiarmid, and A. J. Epstein, Phys. Rev. Lett. **66**, 1745 (1991).

[20]A. G. MacDiarmid and A. J. Epstein, Faraday Discuss. Chem. Soc. **88**, 317 (1989).

[21]See, for example, Proceedings of the International Conference

on the Science and Technology of Synthetic Metals, Tübingen, Germany, 1990, edited by M. Hanack, S. Roth, and H. Schier [Synth. Met. **41-43** (1991)]; Proceedings of the International Confernece on the Science and Technology of Synthetic Metals, Santa Fe, NM, edited by M. Aldissi [Synth. Met. **27-29** (1989)].

[22]F. Zuo, M. Angelopoulos, A. G. MacDiarmid, and A. J. Epstein, Phys. Rev. B **36**, 3475 (1987).

[23]B. Lundberg, W. R. Salaneck, and L. Lundstrom, Synth. Met. **21**, 143 (1987).

[24]F. Wudl, R. O. Angus, F. L. Lu, P. M. Allemand, D. J. Vachon, M. Nowak, Z. X. Liu, and A. J. Heeger, J. Am. Chem. Soc. **109**, 3677 (1987).

[25]K. Mizoguchi, M. Nechtschein, J.-P. Travers, and C. Menardo, Phys. Rev. Lett. **63**, 66 (1989); K. Mizoguchi, M. Nechtschein, and J. P. Travers, *ibid.* **65**, 665 (1990); A. J. Epstein, A. G. MacDiarmid, and J. P. Pouget, *ibid.* **65**, 664 (1990). It is noted that Mizoguchi *et al.* studied the ES-I form of polyaniline, while the data we report here are for the ES-II form (Ref. 26). However, the comparison of our earlier results for $\epsilon(T)$ (Ref. 43) and $\sigma(T)$ (Ref. 22) of unoriented ES-I with those of unoriented ES-II suggests that it is reasonable to apply the conclusions of this study to ES-I as well.

[26]M. E. Józefowicz, R. Laversanne, H. H. S. Javadi, A. J. Epstein, J. P. Pouget, X. Tang, and A. G. MacDiarmid, Phys. Rev. B **39**, 12 958 (1989); J. P. Pouget, M. E. Józefowicz, A. J. Epstein, X. Tang, and A. G. MacDiarmid, Macromolecules **24**, 779 (1991); M. Larandjani, J. P. Pouget, E. M. Scherr, A. G. MacDiarmid, M. Józefowciz, and A. J. Epstein, *ibid.* (to be published).

[27]H. H. S. Javadi, F. Zuo, M. Angelopoulos, A. G. MacDiarmid, and A. J. Epstein, Mol. Cryst. Liq. Cryst. **160**, 225 (1988); H. H. S. Javadi, M. Angelopoulos, A. G. MacDiarmid, and A. J. Epstein, Synth. Met. **26**, 1 (1988); M. Angelopoulos, A. Ray, A. G. MacDiarmid, and A. J. Epstein, *ibid.* **21**, 21 (1987).

[28]Z. H. Wang, H. H. S. Javadi, A. Ray, A. G. MacDiarmid, and A. J. Epstein, Phys. Rev. B **42**, 5411 (1990); Z. H. Wang, A. Ray, A. G. MacDiarmid, and A. J. Epstein, *ibid.* **43**, 4373 (1991).

[29]N. F. Mott and E. Davis, *Electronic Processes in Noncrystalline Materials* (Clarendon, Oxford, 1979).

[30]E. P. Nakhmedov, V. N. Prigodin, and A. N. Samukhin, Fiz. Tverd. Tela (Leningrad) **31**, 64 (1989) [Sov. Phys. Solid State **31**, 368 (1989)].

[31]D. J. Thouless, Phys. Rev. Lett. **39**, 1167 (1977).

[32]M. Cini and P. Ascarelli, J. Phys. F **4**, 1998 (1974).

[33]J. E. Wertz and J. R. Bolton, *Electron Spin Resonance: Elementary Theory and Practical Applications* (McGraw-Hill, New York, 1972).

[34]B. Al'tshuler and B. M. Kozyrev, *Electron Paramagnetic Resonance* (Academic, New York, 1964).

[35]R. Kubo and K. Tomita, J. Phys. Soc. Jpn. **9**, 888 (1954).

[36]M. J. Hennessy, C. D. McElwee, and P. M. Richards, Phys. Rev. B **7**, 930 (1973).

[37]K. R. Cromack, M. E. Józefowicz, J. M. Ginder, R. P. McCall, G. Du, K. Kim, J. M. Leng, C. Li, Z. H. Wang, A. J. Epstein, M. A. Druy, P. J. Glatkowski, E. M. Scherr, and A. G. MacDiarmid, Macromolecules **24**, 4157 (1991); E. M. Scherr, A. G. MacDiarmid, S. K. Manohar, J. G. Masters, Y. Sun, X. Tang, M. A. Druy, P. J. Glatkowski, V. B. Cajibe, J. E. Fischer, K. R. Cromack, M. E. Jozefowicz, J. M. Ginder, R. P. McCall, and A. J. Epstein, Synth. Met. **41**, 735 (1991).

[38]M. E. Jozefowicz, X. Tang, and A. J. Epstein, Synth. Met. (to be published).

[39]P. M. Chaikin and J. F. Kwak, Rev. Sci. Instrum. **46**, 218 (1975).

[40]J. Yue, Z. H. Wang, K. R. Cromack, A. J. Epstein, and A. G. MacDiarmid, J. Am. Chem. Soc. **113**, 2665 (1991). Note that for SPAN, $[SO_3]/[N]=0.50$ so that the polymer charge density is the same as for PAN-ES.

[41]S. L. Zhao, Z. H. Wang, A. J. Epstein, S. K. Manohar, A. G. MacDiarmid, and C. H. Hsu, Bull. Am. Phys. Soc. **36**, 782 (1991).

[42]L. Buravov and I. F. Shchegolev, Prib. Tekh. Eksp. **2**, 171 (1971) [Instrum. Exp. Tech. (USSR) **14**, 528 (1971)].

[43]H. H. S. Javadi, K. R. Cromack, A. G. MacDiarmid, and A. J. Epstein, Phys. Rev. B **39**, 3579 (1989).

[44]Z. H. Wang, E. Ehrenfreund, A. Ray, A. G. MacDiarmid, and A. J. Epstein, Mol. Cryst. Liq. Cryst. **189**, 263 (1990).

[45]P. Vaca *et al.* (unpublished).

[46]G. E. Pake and T. L. Estle, *The Physical Principles of Electron Paramagnetic Resonance* (Benjamin, Reading, 1973).

[47]J. H. Freed, D. S. Leniart, and J. S. Hyde, J. Chem. Phys. **47**, 2762 (1967).

[48]P. Sheng and B. Abeles, Phys. Rev. Lett. **28**, 34 (1972).

[49]B. I. Shklovskii and A. L. Efros, *Electronic Properties of Doped Semiconductors* (Springer-Verlag, Berlin, 1984), pp. 228–243.

[50]K. S. Narayan *et al.* (unpublished). The value 11.6 states/eV per 2 rings is for PAN-ES(II) (Ref. 26), differs from 3.5 states/eV per 2 rings (Ref. 56) for PAN-ES(I) (Ref. 26). Note that PAN-ES(II) is ~20% less compact than PAN-ES(I) (Ref. 26).

[51]E. K. Sichel, M. F. Rubner, M. A. Druy, J. I. Gittleman, and S. Bozowski, Phys. Rev. B **29**, 6716 (1984).

[52]P. A. Lee, T. M. Rice, and P. W. Anderson, Solid State Commun. **14**, 703 (1974).

[53]R. L. Bush, Phys. Rev. B **13**, 805 (1976); M. J. Rice and J. Bernasconi, J. Phys. F **2**, 905 (1972).

[54]I. Webman, J. Jortner, and M. H. Cohen, Phys. Rev. B **16**, 2959 (1977).

[55]H. H. S. Javadi, J. S. Miller, and A. J. Epstein, Phys. Rev. Lett. **59**, 1760 (1987).

[56]J. M. Ginder, A. F. Richter, A. G. MacDiarmid, and A. J. Epstein, Solid State Commun. **63**, 97 (1987).

[57]S. Stafstrom, J. L. Bredas, A. J. Epstein, H. S. Woo, D. B. Tanner, W. S. Huang, and A. G. MacDiarmid, Phys. Rev. Lett. **59**, 1464 (1987).